



A. Wilczek · A. Szadziński · N. Kalantar-Nayestanaki ·
St. Kistryn · A. Kozela · I. Skwira-Chalot · E. Stephan

The Forward-Plane Star in $^1\text{H}(d, pp)n$ Breakup at $E_d = 80$ MeV/nucleon

Received: 30 May 2021 / Accepted: 14 July 2021 / Published online: 24 August 2021
© The Author(s) 2021

Abstract Analysis of the data acquired with the BINA detector system in $^1\text{H}(d, pp)n$ reaction at the beam energy of 80 MeV/nucleon makes a systematic analysis of the star configurations possible. This paper shows the preliminary cross section of the Forward-Plane Star (FPS) configuration with the neighbouring configurations.

1 Introduction

The Space Star Anomaly (SSA) [1], stands for a long-lasting discrepancy between differential cross section measured for deuteron-proton breakup at 13 MeV and the theoretical predictions. The Space Star denotes a specific configuration where the momenta of the reaction products form an equilateral triangle perpendicular to the beam momentum in the centre-of-momentum frame. The analyses for the other star configurations differing from the Space Star by the inclination of the triangle plane to the beam axis (α) showed that the discrepancy disappears with decreasing slope [2].

So far, there are no systematic studies of SSA at intermediate energies. The only dedicated measurement at 65 MeV [3] suggested no anomaly and some increased sensitivity to relativistic effects. A scan over beam energies performed for a broad set of star configurations, including the Space Star, can shed light on the SSA problem and the role of relativistic effects in the description of the breakup reaction. It is interesting to see whether the effect persists at the beam energies around 100 MeV/nucleon.

The first step to complete the program is to measure the reference configurations near the Forward-Plane Star, where the data are expected to follow the theoretical calculations for both low and medium energies.

This project is supported by the National Science Centre, Poland (Grants No. 2016/23/D/ST2/01703, and 2012/05/B/ST2/02556)

A. Wilczek (✉) · A. Szadziński · E. Stephan
Institute of Physics, University of Silesia in Katowice, Chorzow, Poland
E-mail: awilczek@us.edu.pl

N. Kalantar-Nayestanaki
ESRIG, University of Groningen, Groningen, The Netherlands

St. Kistryn
Institute of Physics, Jagiellonian University, Kraków, Poland

A. Kozela
Institute of Nuclear Physics, PAS, Kraków, Poland

I. Skwira-Chalot
Faculty of Physics, University of Warsaw, Warsaw, Poland

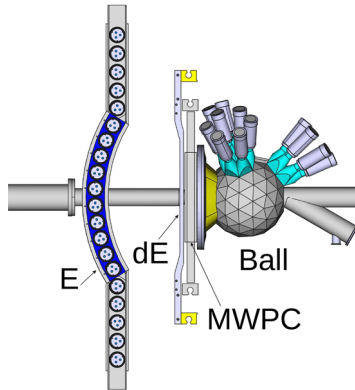


Fig. 1 A schematics of the BINA detector system showing all the active parts. They are (from left to right) the Wall, consisting of a scintillator calorimeter (E), specific energy loss detectors (ΔE), MWPC and the Ball. The beam is coming from the right

2 The BINA Detector System

The experiments performed with BINA at KVI, Groningen, and at CCB, Krakow, make it possible to extend the experimental data on the Space Star cross section with the measurements taken at 50, 80, 108, 135, and 160 MeV/nucleon.

The data were measured with the BINA detector (Fig. 1). For details on the experimental setups see [4]. The target is placed in the very central part of the detector system. It utilises a cryogenic system to liquify the target gas (deuterium or hydrogen) into the volume between two aramid windows glued onto a aluminium frame. The target is surrounded by the Ball. The Ball is an active detector made of 149 phoswich-type scintillator detectors (polyhedrons of triangular cross section) organised in a structure resembling a football ball's surface and a scattering chamber at once. The Ball covers a wide range of angles, $\theta \in (40^\circ, 165^\circ)$, but its angular resolution defined by the size of its elements is about 10° in θ .

The forward angles are covered by the Wall detector, the first part of which is a Multi-Wire Proportional Chamber, responsible for a good angular reconstruction (full azimuthal acceptance: $\theta \in (12^\circ, 30^\circ)$, partial acceptance up to 35° due to the square-formed shape of the MWPC detector, resolution: about 1°). It makes use of 3 detection layers. Optionally, the ΔE detector assembled from 24 vertically placed Bicron BC-408 scintillators can be placed downstream from the MWPC. The most downstream detector is the E detector. It is made of 10 horizontal BC-408 blocks placed on the surface of a target-centred cylinder. The detector makes it possible to stop all the reaction products entirely for the beam energy of 80 MeV/nucleon. The ΔE and E detectors are combined together in order to work as a particle identification system. The experimental threshold for detecting protons is about 20 MeV.

Such a detector system covers a solid angle of almost 4π , which makes the system well-fitted to the measurements of the star geometries. The analyses showed that the Space Star configuration is out of reach for the BINA detector in the case of inverse kinematics, where $\alpha = 90^\circ$ involves polar angles, θ , of $\sim 34^\circ$, for which relative azimuthal angle $\varphi_{12} = 120^\circ$ is out of acceptance, as only φ_{12} angles about 90° and 180° can be measured. The star configurations, the inclination angle of which is not higher than 70° , are accepted. The recently acquired data in normal kinematics (proton incident on deuteron) are well within reach of the experiment. In this case, $\alpha \in [0^\circ, 20^\circ]$ can be measured as Wall-Wall coincidences, $\alpha \in [0^\circ, 50^\circ]$ as Wall-Ball coincidences after rotating them slightly about the axis perpendicular to the reaction plane and $\alpha \in (50^\circ, 180^\circ]$ as Ball-Ball coincidences. The highest precision can be obtained for the configurations where the coincidences do not involve the central part of the detector (Ball), that is, for configurations near the FPS.

3 Results

The analysis of charged deuteron-proton breakup $^1\text{H}(d, pp)n$ -reaction at 80 MeV/nucleon was based upon the paper by Parol et al. [5] and relies on the reconstruction of proton energies, polar angles, and the relative azimuthal angle of the proton pair. The cross section was compared to the theoretical calculations [6, 7]: CD-Bonn with Coulomb potential (CDB+C), CD-Bonn with explicit Δ excitation (CDB+ Δ), and CD-Bonn with

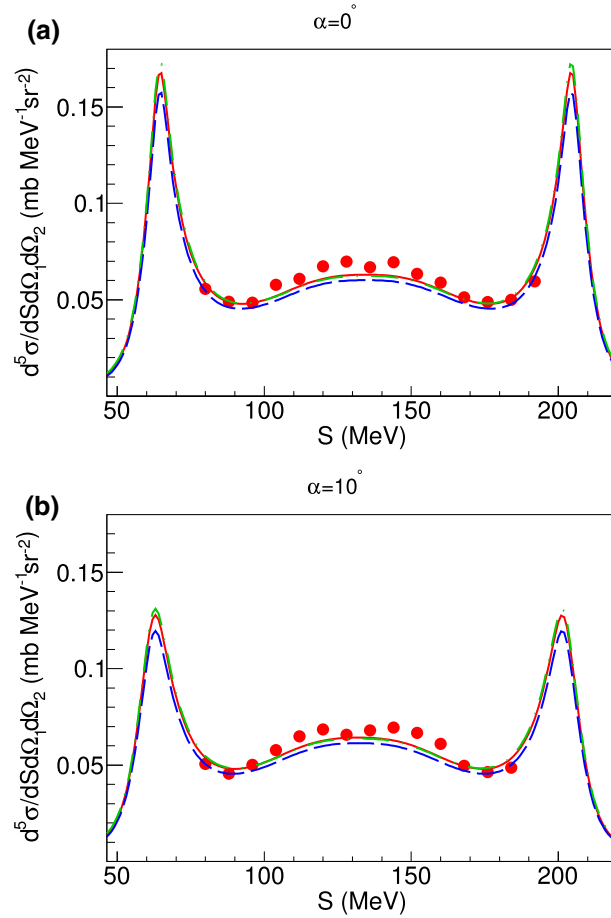


Fig. 2 Cross section for $^1\text{H}(d(160\text{ MeV}), pp)n$ breakup for **a** $\theta_1 = \theta_2 = 23.49^\circ \pm 1^\circ$, and the relative azimuthal angle $\varphi_{12} = 180^\circ \pm 5^\circ$ ($\alpha = 0^\circ$ star configuration), **b** $\theta_1 = \theta_2 = 23.67^\circ \pm 1^\circ$, and $\varphi_{12} = 168.55^\circ \pm 5^\circ$ ($\alpha = 10^\circ$). The data are plotted against arc length measured anti-clockwise along the kinematics (S). The starting point ($S = 0$) is arbitrarily chosen as the point where the energy of the second proton is minimal and starts to increase. The star configuration corresponds to the axis of symmetry of the plot which is around $S = 135$ MeV. Theoretical predictions are plotted as lines (red solid: CD-Bonn+ Δ +Coulomb, green chain: CD-Bonn+ Δ , blue dashed: CD-Bonn+Coulomb). Statistical uncertainty is contained within the marker. Systematic uncertainty (about 7%) is not shown in the plots

both Coulomb and Δ (CDB+ Δ +C). Only two latter potentials contain the three-nucleon force (3NF) effects in addition to a pure 2NF-potential.

The results for $\alpha = 0^\circ$ (FPS) and 10° are shown at the axis of symmetry of the plots in Fig. 2. The figure is obtained for the angular configuration characteristic of the star protons in the laboratory frame of motion. In the case of $\alpha = 0^\circ$ the polar angle of the outgoing protons $\theta_1 = \theta_2 = 23.49^\circ$, and the relative azimuthal angle $\varphi_{12} = 180^\circ$, whilst for $\alpha = 10^\circ$ $\theta_1 = \theta_2 = 23.67^\circ$, and $\varphi_{12} = 168.55^\circ$. The graph is plotted against the length of kinematics (S). The points on the axis of symmetry correspond to the configuration, where the energies of outgoing protons are equal (a star configuration). The points farther away from the symmetry axis correspond to the same angular configurations of the breakup products, but the momenta are less and less equally partitioned. The dashed line stands for CD-Bonn+Coulomb potential (pure 2NF), the chain line for CD-Bonn+ Δ (3NF, no Coulomb), and the solid line for CD-Bonn+ Δ +Coulomb potential (3NF).

The systematic uncertainties for the analysed configurations are estimated to be about 7% [5].

The data show the experiment agrees with the theoretical predictions within the systematic uncertainty. The analysis will be continued in order to obtain data on other configurations within the range of the star inclination angle $\alpha \in [0^\circ; 70^\circ]$ for inverse kinematics, as well as on all α configurations, including the Space Star for normal kinematics, at proton beam energies of 108 and 160 MeV.

Open Access This article is licensed under a Creative Commons Attribution 4.0 International License, which permits use, sharing, adaptation, distribution and reproduction in any medium or format, as long as you give appropriate credit to the original author(s) and the source, provide a link to the Creative Commons licence, and indicate if changes were made. The images or other third party material in this article are included in the article's Creative Commons licence, unless indicated otherwise in a credit line to the material. If material is not included in the article's Creative Commons licence and your intended use is not permitted by statutory regulation or exceeds the permitted use, you will need to obtain permission directly from the copyright holder. To view a copy of this licence, visit <http://creativecommons.org/licenses/by/4.0/>.

References

1. J. Strate et al., Nucl. Phys. A **501**, 51 (1989). [https://doi.org/10.1016/0375-9474\(89\)90564-2](https://doi.org/10.1016/0375-9474(89)90564-2)
2. K. Ohnaka et al., Few-Body Syst. **55**, 725 (2014). <https://doi.org/10.1007/s00601-014-0890-7>
3. J. Zejma et al., Phys. Rev. C **55**, 42 (1997). <https://doi.org/10.1103/PhysRevC.55.42>
4. S. Kistryn, E. Stephan, J. Phys. G **40**, 063101 (2013). <https://doi.org/10.1088/0954-3899/40/6/063101>
5. W. Parol et al., Phys. Rev. C **102**, 054002 (2020). <https://doi.org/10.1103/PhysRevC.102.054002>
6. A. Deltuva, A.C. Fonseca, P.U. Sauer, Phys. Rev. C **72**, 054004 (2005). <https://doi.org/10.1103/PhysRevC.72.054004>
7. A. Deltuva, Phys. Rev. C **80**, 064002 (2009). <https://doi.org/10.1103/PhysRevC.80.064002>

Publisher's Note Springer Nature remains neutral with regard to jurisdictional claims in published maps and institutional affiliations.